DOI: 10.1002/chem.201304315

Metallogels

Supramolecular Polymers Self-Assembled from *trans*-Bis(pyridine) Dichloropalladium(II) and Platinum(II) Complexes

Mingming Chen,[a] Chengsha Wei,[b] Jiaojiao Tao,[a] Xibo Wu,[a] Ningdong Huang,[a] Guobin Zhang,*[a] and Liangbin Li*[a, b]

Abstract: Two structurally similar *trans*-bis(pyridine) dichloropalladium(II)- and platinum(II)-type complexes were synthesized and characterized. They both self-assemble in *n*-hexane to form viscous fluids at lower concentrations, but form metallogels at sufficient concentrations. The viscous solutions were studied by capillary viscosity measurements and UV/Vis absorption spectra monitored during the disassembly process indicated that a metallophilic interaction was involved in the supramolecular polymerization process. For the two supramolecular assemblies, uncommon continuous porous networks were observed by using SEM and TEM revealed that they were built from nanofibers that fused and crosslinked with the increase of concentration. The xerogels of the palladium and platinum complexes were carefully studied by using synchrotron radiation WAXD and EXAFS. The WAXD data show close stacking distances driven by π–π and metal–metal interactions and an evident dimer structure for the platinum complex was found. The coordination bond lengths were extracted from fitting of the EXAFS data. Moreover, close Pt^{II}–Pt^{II} (Pd^{II}–Pd^{II}) and Pt–Cl (Pd–Cl) interactions proposed from DFT calculations in the reported oligo(phenylene ethynylene) (OPE)-based palladium(II) pyridyl supramolecular polymers were also confirmed by using EXAFS. The Pt^{II}–Pt^{II} interaction is more feasible for supramolecular interaction than the Pd^{II}–Pd^{II} interaction in our simple case.

Introduction

Supramolecular systems polymerized through noncovalent secondary interactions have attracted tremendous interest recently.[1] In particular, supramolecular polymers self-assembled from metal complexes are of great use in material science. By tuning the metal–ligand interactions, the rich electronic, magnetic, and photonic properties of metal species can be introduced to supramolecular polymers while maintaining the fascinating self-healing and stimuli-response advantages. Thus they have applications in emissive, photovoltaic, sensing, responsive, healing, and even drug-delivery materials.[2]

Of the various metallosupramolecular systems, the research of d^8 platinum(II), palladium(II), gold(III) complexes has been a hot topic[3] because they show rich photophysical properties and biological applications. In addition, the square-planar geometry of these complexes greatly favors supramolecular interactions. For instance, a series of metallogelators based on rod-like platinum–acetylide complexes, which displayed intriguing photophysical properties, have been reported.[4] In addition, the d^8 complexes are known to show metallophilic interactions. The d–d interactions are very sensitive to external stimuli and are often accompanied by luminescence. Thus they are very promising materials for sensors and displays. Additionally, d–d interactions can play an important part in the assembly process. A representative class is terpyridine platinum(II) complexes as they often aggregate through Pt^{II}–Pt^{II} combined with π–π interactions.[5] A very recently work has also shown that Pd^{II}–Pd^{II} interaction can be the driving force for cooperative supramolecular polymerization.[6] Close metal–metal interactions are often found in the solid state but may be weakened in solution, especially in polar solvents, yet together with other noncovalent interactions, such as π–π stacking, very tough assemblies can often been obtained.

Herein, we report the self-assembly behavior of two structurally similar *trans*-bis(pyridine) dichloropalladium(II)- and platinum(II)-type complexes. Pyridyl ligand **L** has a pyridine head group and a 3,4,5-tris(dodecyloxy)benzene tail linked with an amide bond in the 3-position. The two complexes abbreviated as $[Pt(\mathbf{L})_2Cl_2]$ and $[Pd(\mathbf{L})_2Cl_2]$ both self-assemble in *n*-hexane to form viscous fluids and metallogels. Though Ag^I-based metallogels with a similar ligand have already been studied,[7] the Pt^{II} and Pd^{II} complexes herein have well-defined structures and are charge-neutral. Their self-assembly behaviors are much like the recently reported oligo(phenylene ethynylene) (OPE)-based

---

[a] M. Chen, J. Tao, X. Wu, Dr. N. Huang, Prof. Dr. G. Zhang, Prof. Dr. L. Li
National Synchrotron Radiation Lab and
College of Nuclear Science and Technology
University of Science and Technology of China
No. 96, JinZhai Road, Hefei, Anhui 230026 (China)
Fax: (+86) 551-5141078
E-mail: gbzhang@ustc.edu.cn
lbli@ustc.edu.cn

[b] C. Wei, Prof. Dr. L. Li
CAS Key Laboratory of Soft Matter Chemistry
Department of Polymer Science and Engineering
University of Science and Technology of China

Supporting information for this article is available on the WWW under http://dx.doi.org/10.1002/chem.201304315.

palladium(II) pyridyl supramolecular polymers.[6] The self-assembly of terpyridine Pt^{II}- and Pd^{II}-type complexes has often been reported but to the best of our knowledge *trans*-bis(pyridine) dichloropalladium(II)-type molecules seem to be new. These mononuclear neutral complexes are easy to prepare but have strong supramolecular interactions. Therefore, we started with a simple ligand and further extended the new concept to the corresponding platinum(II) complexes.

Results and Discussion

Complexes $[Pt(\mathbf{L})_2Cl_2]$ and $[Pd(\mathbf{L})_2Cl_2]$ (Figure 1) were prepared by heating ligand **L** at reflux with $PtCl_2$ and $PdCl_2$, respectively, in toluene. All the structures have been successfully characterized by using ^1H NMR spectroscopy and ESI-MS (see the Supporting Information). EXAFS spectra further confirmed the structures and will be analyzed in detail below. The two complexes are only slightly soluble in *n*-hexane at room temperature but highly soluble at 60 °C. Upon cooling, either viscous liquids or metallogels form. Microfibers can be pulled from the viscous solutions (Figure 2a), which indicates strong interactions between the molecules. Metallogels form at sufficiently high concentrations (Figure 2b and c) and $[Pt(\mathbf{L})_2Cl_2]$ has a higher gelation ability than $[Pd(\mathbf{L})_2Cl_2]$. The critical gelation concentration is about 8 mм for $[Pt(\mathbf{L})_2Cl_2]$ but 20 mм for $[Pd(\mathbf{L})_2Cl_2]$. Ligand **L** is highly soluble in *n*-hexane and does not show any aggregation character. Thus, aggregation takes place after coordination.

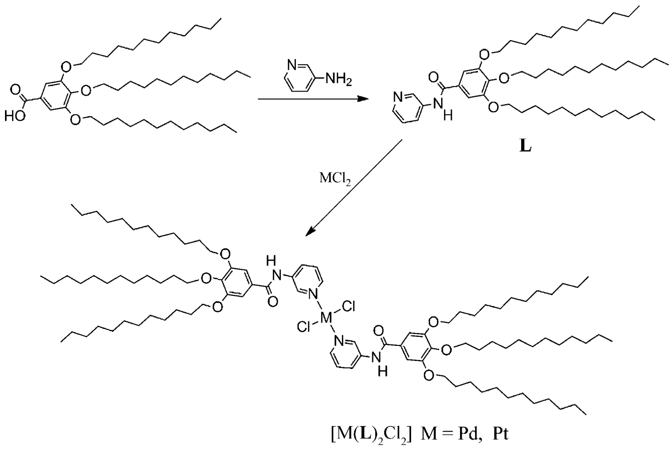

Figure 1. Synthetic route for ligand **L** and the two complexes.

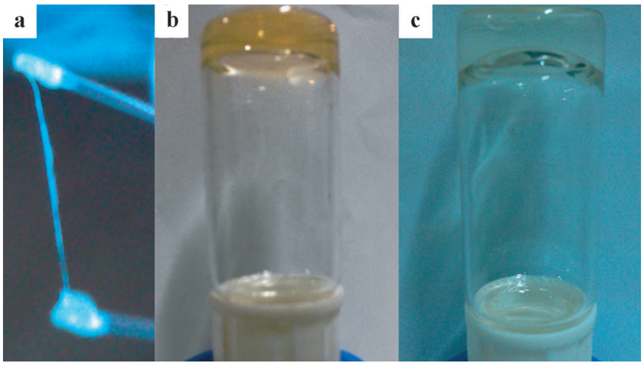

Figure 2. a) A single microfiber pulled between two capillary tubes (inner diameter 0.5 mm) from a viscous solution of $[Pd(\mathbf{L})_2Cl_2]$ (18 mм). b,c) Gel images of $[Pd(\mathbf{L})_2Cl_2]$ (20 mм) and $[Pt(\mathbf{L})_2Cl_2]$ (8 mм), respectively.

The viscous solutions formed by the two complexes have been examined by using capillary viscosity measurements in the concentration range of 0.05 to 1 mм, with the ligand for comparison. The measured specific viscosities of $[Pt(\mathbf{L})_2Cl_2]$ solutions were always higher than the corresponding $[Pd(\mathbf{L})_2Cl_2]$ solutions (Figure 3a). The two log–log plots both show a good linear relationship (Figure 3b). The slopes for $[Pt(\mathbf{L})_2Cl_2]$ and $[Pd(\mathbf{L})_2Cl_2]$ are 1.75 and 1.69, respectively. As the slope for non-interacting species in solution should be close to 1,[8] self-assembly certainly occurs in *n*-hexane. Moreover, supramolecular aggregation abilities could be judged by the slope values[8] and the association constant of $[Pt(\mathbf{L})_2Cl_2]$ is thought to be slightly higher than that of $[Pd(\mathbf{L})_2Cl_2]$. As discussed later, the supramolecular polymerization process follows a cooperative mechanism. The association constant here should belong to the elongation period. This slight advantage cannot be the

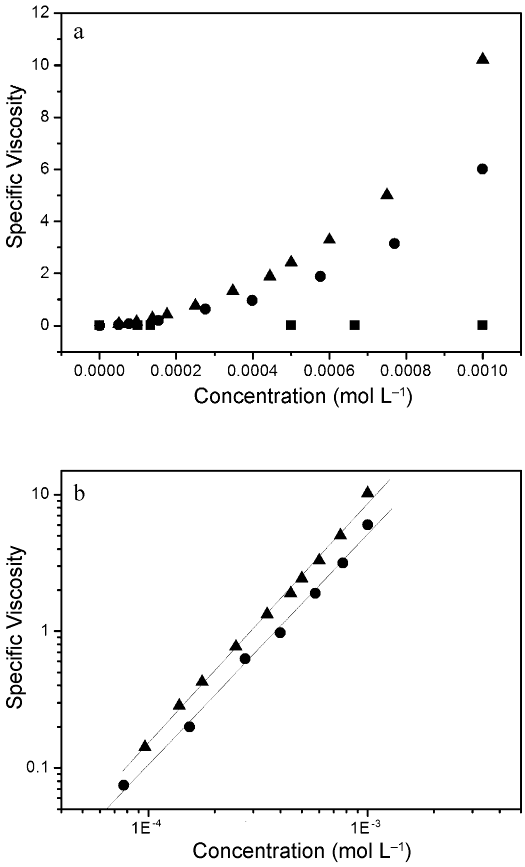

Figure 3. a) Specific viscosity (21 °C) of ligand **L** (■), $[Pt(\mathbf{L})_2Cl_2]$ (▲), and $[Pd(\mathbf{L})_2Cl_2]$ (●) in *n*-hexane and b) the corresponding log–log plots for $[Pt(\mathbf{L})_2Cl_2]$ (▲; slope = 1.75), and $[Pd(\mathbf{L})_2Cl_2]$ (●; slope = 1.69).

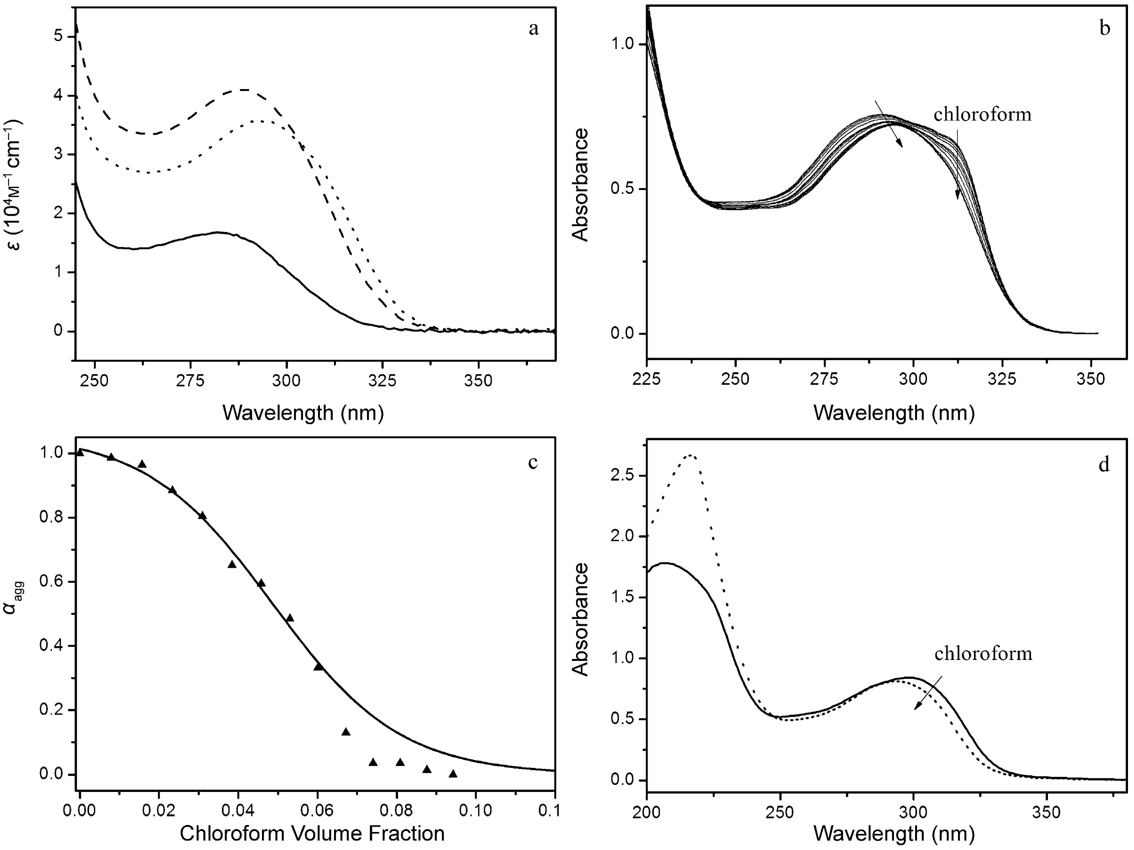

Figure 4. a) UV/Vis spectra of ligand **L** (——), [Pt(**L**)$_2$Cl$_2$] (•••••), and [Pd(**L**)$_2$Cl$_2$] (-----) in chloroform (5×10^{-5} M). b) UV/Vis spectra change due to the disaggregation process upon gradually adding chloroform to solutions of [Pt(**L**)$_2$Cl$_2$] in *n*-hexane. c) The absorbance decrease at $\lambda = 312.6$ nm in (b) deviates from a sigmoidal fitting (isodesmic model). d) UV/Vis spectra change due to the disaggregation process upon adding 10% chloroform to solutions of [Pd(**L**)$_2$Cl$_2$] in *n*-hexane.

sole cause of the large viscosity difference. [Pt(**L**)$_2$Cl$_2$] already takes a lead over [Pd(**L**)$_2$Cl$_2$] in the nucleation period.

The self-assembly mechanisms of [Pt(**L**)$_2$Cl$_2$] and [Pd(**L**)$_2$Cl$_2$] have been inspected by using UV/Vis absorption spectra. The two complexes both showed one broad band in the region from $\lambda = 260$ to 340 nm with some redshift compared to the free ligand in chloroform (Figure 4a). We ascribe this band to π–π* transition of the pyridine group. No obvious MLCT bands appeared because they are often two orders lower in absorbance.[9] In the aggregated state in *n*-hexane (0.6 mM), [Pd(**L**)$_2$Cl$_2$] only showed a redshift of the π–π* band center from $\lambda = 288$ to 294 nm. However, in [Pt(**L**)$_2$Cl$_2$] two peaks centered at $\lambda = 288$ and 312 nm emerged. UV/Vis absorption spectra at elevated temperatures suggested that the shoulder band gradually disappeared, which further confirmed that the new peak at $\lambda = 312$ nm is due to aggregation (Figure S1 in the Supporting Information). For the two complexes, spectra at concentrations of 0.05 and 1 mM were almost identical. Because the 1 mM solutions are quite viscous, aggregation surely takes place. We conclude the two complexes can already self-assemble at a concentration of 0.05 mM in *n*-hexane. This conclusion has also been confirmed by the viscosity measurements. Because more dilute solutions are not suitable for UV/Vis studies, concentration-dependent work is unable. Alternatively, motivated by the recent work of the Meijer group,[10] we have checked the disassembly process by adding a good solvent, chloroform, to the aggregated solutions in *n*-hexane. On addition of chloroform to [Pt(**L**)$_2$Cl$_2$], the peak at $\lambda = 312$ nm gradually disappeared and the peak at $\lambda = 288$ nm shifted to $\lambda = 294$ nm (Figure 4b). A blueshift of the aggregated state reveals a H-type stack of pyridine moieties. The absorbance decrease at $\lambda = 312.6$ nm gives a typically nonsigmoidal shape, which means the aggregating process follows a cooperative mechanism (Figure 4c). For [Pd(**L**)$_2$Cl$_2$], a blueshift of about 8 nm upon addition of 10% percent chloroform was observed (Figure 4d). The increase in solvent polarity generally causes a redshift of the π–π* band, so the blueshift must be generated by disaggregation. Referring to the similar Pd complex,[6] a redshift upon aggregation indicates interaction of the axial d_{z^2} orbitals of the central palladium(II) atoms. Thus although no new band appears, metallophilic interactions do exist.

Electron microscopy observations gave an insight into the microstructures of the aggregates. For [Pt(**L**)$_2$Cl$_2$], nanofibers were observed in dilute solutions by using TEM. As shown in Figure 5a, fibers with diameters around 10 nm formed predominantly at concentrations of 0.25 mM, then fused into much thicker fibers as the concentration was increased to 1 mM (Figure 5b). The fibers observed by TEM were not bun-

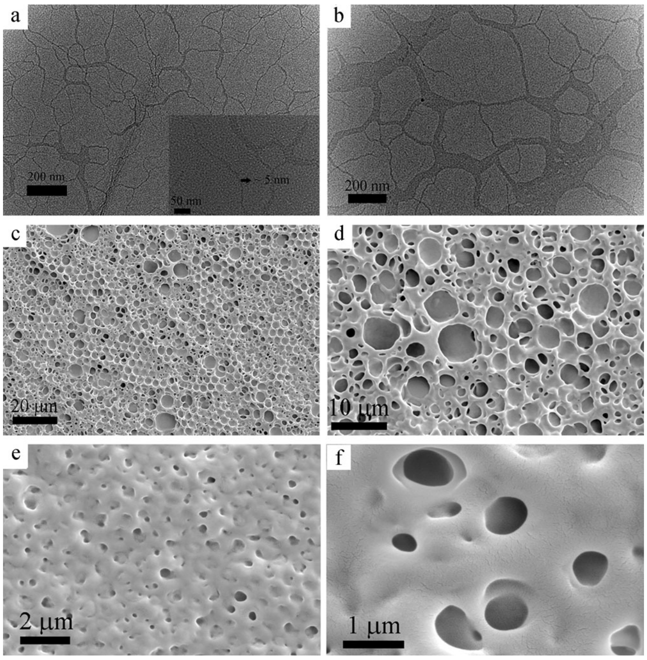

Figure 5. TEM images of freeze-dried solutions of a) 0.25 mm (scale bar: 200 nm; inset scale bar: 50 nm, arrow indicates 5 nm) and b) 1 mm [Pt(**L**)$_2$Cl$_2$] in *n*-hexane and SEM images of freeze-dried solutions of 1 mm [Pt(**L**)$_2$Cl$_2$] (c and d) and 4 mm [Pd(**L**)$_2$Cl$_2$] (e and f).

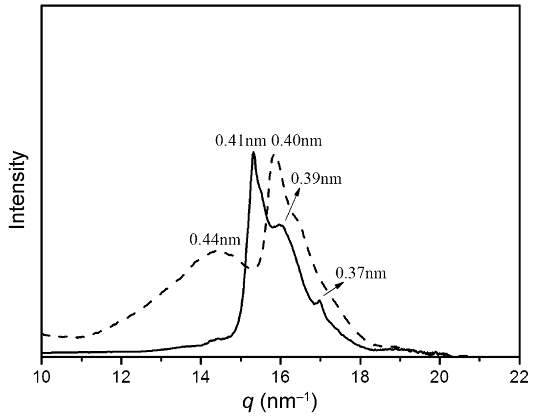

Figure 6. WAXD spectra of xerogels of [Pt(**L**)$_2$Cl$_2$] (——) and [Pd(**L**)$_2$Cl$_2$] (-----), normalized intensity was used.

dles but easily connected with each other to form continuous networks. The diameter of the thinnest fiber observed was about 5 nm, which matches the length of the molecule well (Figure 5a, insert). We concluded that the fibers were grown from columnar stacking of the disc-like molecules. SEM analysis also confirmed the structure of continuous fibrillar networks. At a concentration of 1 mm, highly crosslinked and entangled fibers formed a porous continuous network (Figure 5c and d), and the diameters of the pores were mainly a few micrometers. Though similar structures in metallogels have also been reported by Yam and co-workers,[11] continuous networks were rarely observed. Very recently Yang and co-workers reported a platinum-based gelator that forms uniform honeycomb morphologies in nonpolar solvents; the pore-size distribution reported herein is not as narrow as their example.[12] Interestingly, for all three cases the gelators are all metal complexes with amide linkers and the reason for this is still not clear. The highly porous metal complexes might have some applications in catalysis. Similar continuous fibrillar morphologies were obtained in the case of [Pd(**L**)$_2$Cl$_2$]. For a more concentrated sample (Figure 5e and f), fibers fused more extensively, but pores could still be observed with diameters of less than 1 µm. All the above results indicated that the two complexes self-assemble through columnar stacking into nanofibers in *n*-hexane and then further crosslink and entangle to form continuous networks and immobilize the solvents.

To further discover how the nanofibers are generated, the xerogels were analyzed by using synchrotron radiation WAXD. As expected, for both samples a few diffraction peaks related to π–π stacking were observed (Figure 6). For [Pd(**L**)$_2$Cl$_2$], a very broad diffraction centered at $d=0.44$ nm and another sharper peak centered at $d=0.40$ nm were observed. For [Pt(**L**)$_2$Cl$_2$], a relatively broad diffraction centered at $d=0.39$ nm was also found. The *d* values of the two sharper peaks were 0.41 and 0.37 nm. Columnar stacking of molecules with peripheral long aliphatic chains often leads to broad diffractions caused by packing of the alkyl groups, and the stacking of central cores gives rise to sharp diffractions.[13] Therefore, the central core of [Pt(**L**)$_2$Cl$_2$] stacks with two different distances and the peripheral long aliphatic chains give only one broad diffraction peak because they are too bulky. Now it is clear that the growth of nanofibers of [Pt(**L**)$_2$Cl$_2$] is through a dimer formation and elongation process, and the shorter diffraction distance corresponds to the dimer space. The results match the UV/Vis analysis well because the aggregation of [Pt(**L**)$_2$Cl$_2$] follows a cooperative (nucleation and growth) mechanism. For platinum(II) complexes, dimer structures have been often reported due to Pt^{II}–Pt^{II} interactions.[5a,14] The same case was found for OPE-based palladium(II) pyridyl dichloride supramolecular polymers.[6] However, no evident dimer structure was observed for [Pd(**L**)$_2$Cl$_2$]. In addition, the [Pd(**L**)$_2$Cl$_2$] xerogel features less-ordered structures than the corresponding [Pt(**L**)$_2$Cl$_2$] xerogel because the peaks are relatively broader. By comparing the *d* values of the two xerogels, we can see that [Pt(**L**)$_2$Cl$_2$] dimers are more tightly stacked. So it is evident that a Pt^{II}–Pt^{II} interaction is more feasible for supramolecular assembly than a Pd^{II}–Pd^{II} interaction, at least in this case. This is why [Pt(**L**)$_2$Cl$_2$] supramolecular polymers in *n*-hexane have higher viscosity and a lower gelation concentration. Because the OPE-based palladium(II) pyridyl dichloride supramolecular polymers clearly showed a Pd^{II}–Pd^{II} interaction (about 0.35 nm),[6] we can also conclude that extended conjugated systems favor metallophilic interactions.

The two xerogels were analyzed in EXAFS experiments. The Fourier transforms (FTs) of $k^3\chi(k)$ EXAFS data is dominated by two intense N and Cl scattering peaks. To get precise coordination bond lengths, the first coordination spheres of M–N and M–Cl shells were fitted. The fitted FTs are shown in Figure 7 and the results are listed in Table 1. The fitted bond lengths are very close to similar ones reported for single-crystal struc-

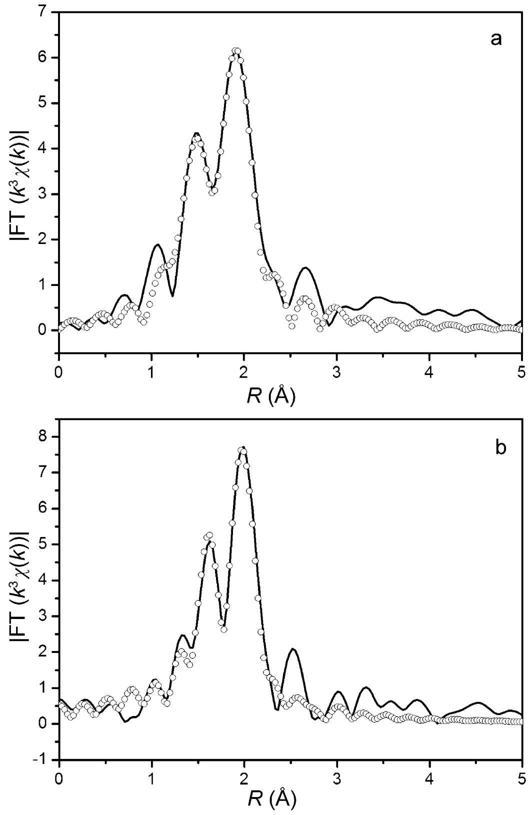

Figure 7. $k^3\chi(R)$ of the EXAFS data in R space for a) [Pd(**L**)$_2$Cl$_2$] and b) [Pt(**L**)$_2$Cl$_2$] xerogels and fitting of the first coordination spheres (○, R range = 1–2.5 Å for [Pd(**L**)$_2$Cl$_2$] and 1–2.3 Å for [Pt(**L**)$_2$Cl$_2$]).

Table 1. Structural parameters extracted from the first coordination sphere EXAFS curve fitting.

	Bond	N[a]	R [Å][b]	σ^2 [Å^2][c]
[Pt(**L**)$_2$Cl$_2$]	Pt–N	2	2.01(1)	0.0022(9)
	Pt–Cl	2	2.30(1)	0.0027(5)
[Pd(**L**)$_2$Cl$_2$]	Pd–N	2	2.01(2)	0.0024(1)
	Pd–Cl	2	2.31	0.0029(1)

[a] The coordination number, was set as a constant. [b] Interatomic distance R. [c] Debye–Waller factor σ^2.

tures,[9,15] which also indicates that the two complexes are typically *trans*-palladium(II) and -platinum(II) bis(pyridine) dichloride complexes. To further analyze the EXAFS spectra, the theoretical scattering paths of a similar *trans*-dichloroplatinum(II) bis(pyridine) single-crystal structure was calculated (Figure S4 in the Supporting Information). In the R region up to 4 Å, there are other two Pt–C single scattering pathways (Figure S4, paths 1 and 2, in the Supporting Information). Strong multiple scatterings from Pt-N-C and Pt-C-C (Figure S4, paths 4 and 5, in the Supporting Information) are expected and the effective distances are similar to Pt–C single scattering path 2. Fortunately, the Pt-N-C multiple scattering (path 3) with a shorter effective distance is almost negligible. This is reasonable because the Pt-N-C angle in path 3 is much smaller than the other two. The effective distances of paths 2, 4, and 5 are all around 4.3 Å, thus we were able to avoid them by fitting R below 3.5 Å in the FTs.

With the theoretical calculation in mind, we have checked the whole FT of [Pt(**L**)$_2$Cl$_2$]. The peak centered at 2.52 Å could be ascribed to the Pt–C shell (path 1), but the other two peaks in the range of 2.8 to 3.5 Å were not expected. From the cooperative growing model of [Pt(**L**)$_2$Cl$_2$], short Pt^{II}–Pt^{II} interactions are responsible for these peaks. Based on the WAXD data, we can use a dimer model to fit the FTs from 1 t 3.5 Å. A Pt–Pt shell surely exists but other shells are also expected. When two platinum atoms closely contact, one chloride atom of the second molecule can also reach a close contact with the first platinum atom. According to the recently reported OPE-based palladium(II) pyridyl gelator, a short Pd–Cl separation also exists in the dimer, which is comparative to the Pd–Pd separation.[6] Therefore, a Pt–Cl shell should also be considered. With this dimer model, the spectra in the R range of 1 to 3.5 Å were fitted (Figure 8). The results are shown in Table 2. EXAFS data indicate that a dimer forms through close contact of Pt–Pt and Pt–Cl of about 3.4 Å. However, more accurate lengths for these supramolecular interactions are difficult to determine. The increased disorder at high R strongly weakens the scattering peaks, which is easily shown from the fitted Debye–Waller factors. Moreover, overlap of other shells and also multiple scat-

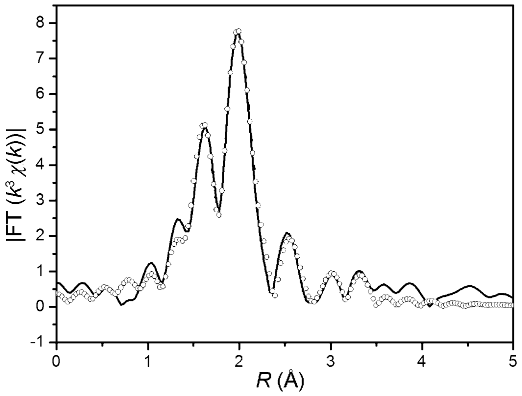

Figure 8. Fitting of $k^3\chi(R)$ of the EXAFS data for [Pt(**L**)$_2$Cl$_2$] in R space (○, R range = 1–3.5 Å).

Table 2. Structural parameters extracted from EXAFS curve fitting in the range of 1–3.5 Å.

	Bond	N	R [Å]	σ^2 [Å^2]
[Pt(**L**)$_2$Cl$_2$]	Pt–N	2	1.99(1)	0.0028(3)[b]
	Pt–Cl	2	2.32(1)	
	Pt–C	4	2.96	0.006(2)
	Pt1–Pt2[a]	1	3.43(9)	0.007(2)
	Pt1–Cl2[a]	1	3.38(5)	0.01

[a] 1 and 2 correspond to atoms of the first or second molecules in a dimer model. [b] Identical values were used for neighboring shells to simplify the curve fitting.

tering add to the difficulty. Thus though the diffraction peak from the WAXD data does not correspond to the direct Pt–Pt contact, the EXAFS Pt–Pt separation seems a little shorter. In any case, close Pt–Pt and Pt–Cl interactions have been confirmed. For $[Pd(\mathbf{L})_2Cl_2]$ the overlap is more complex and we were not able to fit the EXAFS spectrum. By simply comparing the two FTs, we can deduce that the supramolecular interactions in $[Pd(\mathbf{L})_2Cl_2]$ are of longer separations and more disorder. EXAFS studies of metal–metal interactions have been rarely reported and sometimes ambiguous results have been obtained.[16] For supramolecular systems, single crystals are often impossible to get and EXAFS remains a powerful tool for analysis. Efforts should be made to enhance the scatterings of relatively longer separations and distinguish them from other shells. The characterization of metallosupramolecular interactions with EXAFS is still ongoing.

Conclusion

We have synthesized two *trans*-bis(pyridine) dichloropalladium(II)- and platinum(II)-type complexes and studied their self-assembly behavior. Supramolecular polymers were formed in *n*-hexane as demonstrated by viscosity measurements. TEM and SEM studies further showed nanofibers that fuse into porous interconnected networks. Generally, the aggregation mechanism of the two complexes is similar. The Van der Waals and hydrogen bonding together with π–π stacking may all assist the self-assembly process. Given the big difference between the viscosity and gelation ability of the two complexes, metal–metal interactions must play a crucial role, which has been confirmed by UV/Vis, WAXD, and EXAFS experiments. A series of similar organic molecules without coordinated metal ions has already been explored and do not show such strong interactions as compared to the systems described herein.[17] After incorporation of square-planar-coordinated metal ions, supramolecular interactions are greatly favored. In our case, the Pt^{II}–Pt^{II} interaction showed an advantage over the Pd^{II}–Pd^{II} interaction. However, with the assistance of extended conjugated systems, strong aggregates could also be obtained for such palladium complexes. Our results have proved that *trans*-bis(pyridine) dichloropalladium(II)- and platinum(II)-type complexes are very promising candidates for the construction of supramolecular assemblies.

Experimental Section

Experimental methods

Tetrahydrofuran (THF), chloroform, toluene and pyridine were distilled under reduced pressure over calcium hydride and then stored over 4 Å molecular sieves. 3,4,5-Tris(dodecyloxy)benzoic acid was prepared according to a reported method.[18] All other reagents and solvents are commercially available and were used as received.

UV/Vis absorption spectra were recorded by using a Shimadzu UV-2401 spectrophotometer. Quartz cells with 1 cm or 0.1 cm path lengths were used to fit the various concentrations. ^1H NMR spectra were obtained at 400 MHz by using a Bruker AV400 NMR spectrometer. Mass spectrum data were obtained by using a Thermo LTQ instrument operated in electrospray ionization (ESI) mode, and both positive and negative spectra were measured. Transmission electron microscopy (TEM) observations were carried out by using a JEM-2100F electron microscope operated at 200 kV. Scanning electron microscopy (SEM) investigations were conducted by using a Philips XL-30-ESEM TMP electron microscope. Viscosity measurements were carried out at 21 °C in *n*-hexane by using a Ubbelohde viscometer.

Wide-angle X-ray diffraction (WAXD) measurements were carried out at the beamline (BL16B1) of the Shanghai Synchrotron Radiation Facility (SSRF). The X-ray wavelength was 0.124 nm and a Mar165 CCD detector (2048 × 2048 pixels with pixel size 80 μm) was employed to collect two-dimensional WAXD patterns. The sample-to-detector distance was calibrated by using CeO_2 powder. Fit2D software from the European Synchrotron Radiation Facility was used to analyze the WAXD patterns in terms of the scattering vector $q = 4\pi\sin\theta/\lambda$ with 2θ as the scattering angle and λ as the X-ray wavelength.

Pd K-edge and Pt L_3-edge EXAFS spectra were measured at the BL14W1 beamline of the Shanghai Synchrotron Radiation Facility (SSRF). A Si(311) double crystal monochromator was used. Data were collected in transmission mode by using ion chambers with mixed nitrogen and argon gas. The standard processing of EXAFS spectra (background removal, Fourier transformation, and nonlinear fitting) was performed by using the ATHENA and ARTEMIS programs of IFFEFIT.[19] Fourier transformation was performed over a range of 3.4–13.5 $Å^{-1}$ (Pd K-edge data) or 2.8–15.6 $Å^{-1}$ (Pt L_3-edge data) with Hanning window functions. The theoretical phase and amplitude functions for single and multiple scattering within a similar molecular model were calculated by using ab initio methods in the FEFF6 program code.[20] The fitting procedure was performed in *R* space. The inelastic reduction factor S_0^2 was extracted from standard Pd and Pt foils. For each coordination, the coordination number *N* was fixed as constant and the interatomic distance *R*, the Debye–Waller factor σ^2, and the edge-energy shift $\triangle E_0$ were fitted.

Synthesis of L

3,4,5-Tris(dodecyloxy)benzoic acid (1.35 g, 2 mmol) was dissolved in chloroform (50 mL) and cooled with ice. Oxalyl chloride (1.27 g, 10 mmol) was added dropwise and then a drop of DMF was added. The solution was stirred for 4 h and the solvent was distilled under vacuum. The dried 3,4,5-tris(dodecyloxy)benzoyl chloride was dissolved in THF (50 mL) and cooled with ice. A solution of 3-amino pyridine (0.28 g, 3 mmol) and pyridine (2 mL) in THF (15 mL) was added dropwise. The resulting mixture was stirred overnight and the poured into water (250 mL). The precipitate was collected and recrystallized from THF/H_2O to give **L** as a white solid (0.98 g, 65 %). ^1H NMR ($CDCl_3$ 400 MHz): $\delta = 8.96$ (s, 1H; PyH), 8.47 (s, 1H; PyH), 8.35 (d, 1H; PyH), 7.44 (q, 1H; PyH), 7.16 (s, 2H; ArH), 4.05 (m, 6H; OCH_2), 1.80 (m, 6H; CH_2), 1.47 (m, 6H; CH_2), 1.26 (m, 48H; CH_2), 0.88 ppm (t, 9H; CH_3); ESI-MS: *m/z* calcd for $C_{48}H_{83}N_2O_4$: 752.18; found: 751.71 $[M+H]^+$.

Synthesis of $[Pd(L)_2Cl_2]$

Palladium dichloride (177 mg, 1 mmol) and **L** (1.50 g, 2 mmol) in toluene (50 mL) were heated at reflux for 4 h, then the solvents were removed by vacuum. The residue was purified by using column chromatography on silica gel (eluent $CHCl_3$/petroleum ether (2:1)) to afford a yellow powder (0.8 g, 48 %). ^1H NMR ($CDCl_3$ 400 MHz): $\delta = 9.47$ (s, 2H; CONH), 8.69 (d, 2H; PyH), 8.57 (s, 2H;

PyH), 8.21 (d, 2 H; PyH), 7.15 (s, 4 H; ArH), 6.98 (q, 2 H; PyH), 4.08 (m, 12 H; OCH_2), 1.80 (m, 12 H; CH_2), 1.48 (m, 12 H; CH_2), 1.26 (m, 96 H; CH_2), 0.88 ppm (t, 18 H; CH_3); ESI-MS (positive-ion mode): *m/z* calcd for $C_{98}H_{168}C_{l2}N_5O_8Pd$: 1721.74; found: 1722.17 $[M+CH_3CN+H]^+$; ESI-MS (negative-ion mode): *m/z* calcd for $C_{96}H_{164}C_{l3}N_4O_8Pd$: 1715.13; found: 1714.80 $[M+Cl]^-$.

Synthesis of $[Pt(L)_2Cl_2]$

Platinum dichloride (266 mg, 1 mmol) and **L** (1.50 g, 2 mmol) in toluene (50 mL) were heated at reflux for 4 h, then the solution was cooled and filtered. The solvents of the filtrate were removed by vacuum and the residue was washed with ethyl acetate and purified by using column chromatography on silica gel (eluent $CHCl_3$/petroleum ether (3:1)) to give a light green powder (0.62 g, 35 %). ^{1}H NMR ($CDCl_3$ 400 MHz): $\delta=9.76$ (s, 2 H; CONH), 8.97 (s, 2 H; PyH), 8.88 (d, 2 H; PyH), 8.27 (d, 2 H; PyH), 7.24 (s, 4 H; ArH), 7.08 (q, 2 H; PyH), 4.08 (m, 12 H; OCH_2), 1.80 (m, 12 H; CH_2), 1.48 (m, 12 H; CH_2), 1.26 (m, 96 H; CH_2), 0.88 ppm (t, 18 H; CH_3); ESI-MS (positive-ion mode): *m/z* calcd for $C_{98}H_{168}C_{l2}N_5O_8Pt$: 1810.40; found: 1810.46 $[M+CH_3CN+H]^+$; ESI-MS (negative-ion mode): *m/z* calcd for $C_{96}H_{164}Cl_3N_4O_8Pt$: 1803.79; found: 1803.30 $[M+Cl]^-$; *m/z* calcd for $C_{96}H_{163}C_{l2}N_4O_8Pt$: 1767.33; found: 1767.25 $[M-H]^-$.

Acknowledgements

This work is supported by the National Natural Science Foundation of China (51325301, U1232129, 11275205, and 11204285), the 973 program of MOST (2010CB 934504), a special financial grant from the China postdoctoral science foundation (2012M521255), the Fundamental Research Funds for the Central Universities (WK2310000025), and the experimental fund of Shanghai Synchrotron Radiation Facility (SSRF).

Keywords: metallogels · metal–metal interactions · palladium · platinum · supramolecular polymers

[1] a) T. Aida, E. W. Meijer, S. I. Stupp, *Science* **2012**, *335*, 813–817; b) F. Huang, O. A. Scherman, *Chem. Soc. Rev.* **2012**, *41*, 5879–5880; c) T. F. A. de Greef, M. M. J. Smulders, M. Wolffs, A. P. H. J. Schenning, R. P. Sijbesma, E. W. Meijer, *Chem. Rev.* **2009**, *109*, 5687–5754.

[2] a) M. O. M. Piepenbrock, G. O. Lloyd, N. Clarke, J. W. Steed, *Chem. Rev.* **2010**, *110*, 1960–2004; b) G. R. Whittell, M. D. Hager, U. S. Schubert, I. Manners, *Nat. Mater.* **2011**, *10*, 176–188; c) M. Burnworth, T. Liming, K. R. Justin, D. J. Andrew, F. L. Beyer, G. L. Fiore, S. J. Rowan, C. Weder, *Nature* **2011**, *472*, 334–338; d) S.-i. Kawano, N. Fujita, S. Shinkai, *J. Am. Chem. Soc.* **2004**, *126*, 8592–8593; e) J.-J. Zhang, W. Lu, R. W. Y. Sun, C.-M. Che, *Angew. Chem.* **2012**, *124*, 4966–4970; *Angew. Chem. Int. Ed.* **2012**, *51*, 4882–4886; f) A. Kishimura, T. Yamashita, K. Yamaguchi, T. Aida, *Nat. Mater.* **2005**, *4*, 546–549.

[3] a) I. Eryazici, C. N. Moorefield, G. R. Newkome, *Chem. Rev.* **2008**, *108*, 1834–1895; b) W.-W. Yam, K. M.-C. Wong, *Chem. Commun.* **2011**, *47*, 11579–11592.

[4] a) T. Cardolaccia, Y. Li, K. S. Schanze, *J. Am. Chem. Soc.* **2008**, *130*, 2535–2545; b) J. Zhang, X. D. Xu, L. J. Chen, Q. Luo, N. W. Wu, D. X. Wang, X. L. Zhao, H. B. Yang, *Organometallics* **2011**, *30*, 4032–4038; c) L. J. Chen, J. Zhang, J. He, X. D. Xu, N. W. Wu, D. X. Wang, Z. Abliz, H. B. Yang, *Organometallics* **2011**, *30*, 5590–5594; d) Y. J. Tian, E. W. Meijer, F. Wang, *Chem. Commun.* **2013**, *49*, 9197–9199.

[5] a) V. W. W. Yam, K. M. C. Wong, N. Zhu, *J. Am. Chem. Soc.* **2002**, *124*, 6506–6507; b) F. Camerel, R. Ziessel, B. Donnio, C. Bourgogne, D. Guillon, M. Schmutz, C. Iacovita, J.-P. Bucher, *Angew. Chem.* **2007**, *119*, 2713–2716; *Angew. Chem. Int. Ed.* **2007**, *46*, 2659–2662; c) W. Lu, Y. Chen, V. A. L. Roy, S. S.-Y. Chui, C.-M. Che, *Angew. Chem.* **2009**, *121*, 7757–7761; *Angew. Chem. Int. Ed.* **2009**, *48*, 7621–7625; d) C. Po, A. Y.-Y. Tam, K. M.-C. Wong, V. W.-W. Yam, *J. Am. Chem. Soc.* **2011**, *133*, 12136–12143.

[6] M. J. Mayoral, C. Rest, V. Stephanenko, J. Schellheimer, R. Q. Albuqerque, G. Fernández, *J. Am. Chem. Soc.* **2013**, *135*, 2148–2151.

[7] Q. Liu, Y. Wang, W. Li, L. Wu, *Langmuir* **2007**, *23*, 8217–8223.

[8] a) F. Wang, C. Y. Han, C. L. He, Q. Z. Zhou, J. Q. Zhang, C. Wang, N. Li, F. H. Huang, *J. Am. Chem. Soc.* **2008**, *130*, 11254–11255; b) J. B. Beck, J. M. Ineman, S. J. Rowan, *Macromolecules* **2005**, *38*, 5060–5068.

[9] A. Krogul, J. Cedrowski, K. Wiktorska, W. P. Ozimi'nski, J. Skupi'nska, G. Litwinienko, *Dalton Trans.* **2012**, *41*, 658–666.

[10] P. A. Korevaar, C. Schaefer, T. F. A. de Greef, E. W. Meijer, *J. Am. Chem. Soc.* **2012**, *134*, 13482–13491.

[11] S.-T. Lam, G.-X. Wang, V. W.-W. Yam, *Organometallics* **2008**, *27*, 4545–4548.

[12] X. D. Xu, J. Zhang, L. J. Chen, X. L. Zhao, D. X. Wang, H. B. Yang, *Chem. Eur. J.* **2012**, *18*, 1659–1667.

[13] a) B. Mohr, G. Wegner, K. Ohta, *J. Chem. Soc. Chem. Commun.* **1995**, 995–996; b) W. Lu, Y.-C. Law, J. Han, S. S.-Y. Chui, D.-L. Ma, N. Zhu, C.-M. Che, *Chem. Asian J.* **2008**, *3*, 59–69.

[14] a) H. K. Yip, L. K. Cheng, K. K. Cheung, C. M. Che, *J. Chem. Soc. Dalton Trans.* **1993**, 2933–2938; b) J. A. Bailey, M. G. Hill, R. E. Marsh, V. M. Miskowski, W. P. Schaefer, H. B. Gray, *Inorg. Chem.* **1995**, *34*, 4591–4599.

[15] A. N. Chernyshev, N. A. Bokach, Y. A. Izotova, M. Haukka, *Acta. Cryst. Sect. E* **2009**, *65*, m60.

[16] a) N. Carr, J. G. Crossley, A. J. Dent, J. R. Gouge, G. N. Greaves, P. S. Jarrett, A. G. Orpen, *J. Chem. Soc. Chem. Commun.* **1990**, 1369–1371; b) D. Ellis, L. J. Farrugia, P. Wiegeleben, J. G. Crossley, A. G. Orpen, P. N. Waller, *Organometallics* **1995**, *14*, 481–488; c) H. de La Riva, A. Pintado-Alba, M. Nieuwenhuyzen, C. Hardacre, M. C. Lagunas, *Chem. Commun.* **2005**, 4970–4972; d) E. J. Fernández, C. Hardacre, A. Laguna, M. C. Lagunas, J. M. López-de-Luzuriaga, M. Monge, M. Montiel, M. E. Olmos, R. C. Puelles, E. Sánchez-Forcada, *Chem. Eur. J.* **2009**, *15*, 6222–6233.

[17] a) C. Xue, X. Weng, J.-J. Ge, Z. Shen, H. Shen, M. J. Graham, K.-U. Jeong, H. Huang, D. Zhang, M. Guo, F. W. Harris, S. Z. D. Cheng, *Chem. Mater.* **2004**, *16*, 1014–1025; b) H. Shen, K.-U. Jeong, M. J. Graham, S. Leng, J. X. Zheng, H. Huang, M. Guo, F. W. Harris, S. Z. D. Cheng, *Soft Matter* **2006**, *2*, 232–242.

[18] E. Terazzi, S. Torelli, G. Bernardinelli, J.-P. Rivera, J.-M. Blnech, C. Bourgogne, B. Donnio, D. Guillon, D. Imbert, J.-C. G. Bunzli, A. Pinto, D. Jeannerat, C. Piguet, *J. Am. Chem. Soc.* **2005**, *127*, 888–903.

[19] B. Ravel, M. Newville, *J. Synchrotron Rad.* **2005**, *12*, 537–541.

[20] M. Newville, *J. Synchrotron Rad.* **2001**, *8*, 322–324.

Received: November 4, 2013